ARTICLE

Expression of the Two Isoforms of the Vesicular Monoamine Transporter (VMAT1 and VMAT2) in the Endocrine Pancreas and Pancreatic Endocrine Tumors

Martin Anlauf, Rolf Eissele, Martin K.-H. Schäfer, Lee E. Eiden, Rudolf Arnold, Ursula Pauser, Günter Klöppel, and Eberhard Weihe

Department of Molecular Neuroscience, Institute of Anatomy and Cell Biology, Philipps University of Marburg (MA,MKHS,EW); the Department of Gastroenterology and Endocrinology, Philipps University of Marburg (RE,RA), Marburg, Germany; the Section on Molecular Neuroscience, Laboratory of Cellular and Molecular Regulation, National Institute of Mental Health, NIMH, Bethesda, Maryland (LEE); and the Department of Pathology, University of Kiel, Kiel, Germany (MA,UP,GK)

SUMMARY The uptake of monoamines into the secretory granules of monoamine-storing neuroendocrine cells is mediated by vesicular monoamine transporter protein 1 or 2 (VMAT1 or VMAT2). This study analyzed the expression of VMAT1 and VMAT2 in endocrine cells of normal human and monkey pancreas. The expression of VMAT1 and VMAT2 was also examined in infants with hyperinsulinemic hypoglycemia and in adults with pancreatic endocrine tumors (PETs). Using immunohistochemistry (IHC) and in situ hybridization (ISH), we demonstrated the mutually exclusive expression of VMAT1 in endocrine cells of the duct system and of VMAT2 in many cells of the islets of Langerhans. By confocal laser scanning microscopy, VMAT1-positive cells were identified as enterochromaffin (EC) cells and VMAT2-positive cells as β-cells. In PETs, VMAT1 was found exclusively in all serotonin-containing tumors. In contrast, VMAT2 expression was lost in many insulinomas, independent of their biological behavior. VMAT2 was expressed by some non-insulin-producing tumors. The mutually exclusive expression of VMAT1 in EC cells and of VMAT2 in β-cells suggests that both cell types store monoamines. Monoamine storage mediated by VMAT1 in EC cells is apparently maintained in EC cell tumors. In contrast, many insulinomas appear to lose their ability to accumulate monoamines via VMAT2.   **(J Histochem Cytochem 51:1027–1040, 2003)**

GASTROENTEROPANCREATIC MOTILITY and secretion are mediated by neurons and neuroendocrine cells, which accumulate and release pepide hormones and biogenic amines. The GI endocrine system is the largest endocrine organ of the body. More than 16 different types of endocrine cells are present in the GI tract (Hakanson et al. 1978; Walsh 1994; Sundler and Hakanson 1988; Anlauf et al. 2000). Each subpopulation has a distinct distribution along the gut. In the oxyntic mucosa of the stomach, the predominant endocrine cell is the histamine-producing enterochromaffin-like (ECL) cell. In the small and large intestine, serotonin-contain-

ing enterochromaffin (EC) cells represent the majority of endocrine cells.

These biogenic amine-containing neuroendocrine cells express specific proteins that enable them to store and secrete monoamines. These include plasma membrane transporters that scavenge and recycle monoamines from the extracellular space and intracellular membrane transporters for monoamine uptake and storage in secretory granules. Visualization of monoamine uptake mechanisms in neuroendocrine cells provides insights into their cell differentiation during development and in transformed cells and enables the role of monoamine-storage mechanisms to be studied in both neoplastic and non-neoplastic disease.

The uptake of monoamines from the cytoplasm into secretory granules is mediated by vesicular monoamine transporters (VMATs) and requires an ATPase-generated proton gradient (Erickson et al. 1996; Eiden

2000; Erickson and Varoqui 2000; Eiden et al. 2002). Two isoforms of the vesicular monoamine transporter (VMAT1 and VMAT2) have been characterized in rodent and human tissue (Erickson et al. 1992; Liu et al. 1992; Erickson and Eiden 1993). Extensive studies employing IHC and ISH have shown that these two transporters are differentially expressed in monoamine-handling cells of the central nervous system, the autonomic nervous system, the hematopoietic system, and the neuroendocrine cell system. The expression of the two transporters in a given cell type is usually, but not always, mutually exclusive (Weihe et al. 1994; Peter et al. 1995; Erickson et al. 1996; Fon et al. 1997; Hansson et al. 1998; Schütz et al. 1998; Eiden 2000; Weihe and Eiden 2000; Eiden et al. 2002).

VMAT1 is expressed in the serotonin-producing EC cells throughout the GI tract, and VMAT2 in the histamine-accumulating ECL cells of the oxyntic mucosa of the stomach (Weihe et al. 1994; Peter et al. 1995; Erickson et al. 1996; Hansson et al. 1998; Schütz et al. 1998). VMAT1 and VMAT2 are therefore excellent markers for identification of GI neuroendocrine tumors deriving from EC cells and ECL cells, respectively (Eissele et al. 1999; Rindi et al. 2000; Jakobsen et al. 2001).

The differential expression of VMAT1 and VMAT2 in the normal endocrine pancreas has never been examined in detail. Therefore, the question of whether VMAT1 and 2 are also useful in distinguishing among tumors originating from the pancreas is still open, although VMAT1 and VMAT2 protein expression in a small number of pancreatic endocrine tumors has been previously examined (Rindi et al. 2000; Jakobsen et al. 2001).

The aim of this study was to investigate VMAT1 and VMAT2 gene expression in the normal human and non-human primate pancreas by radioactive ISH and to determine the hormonal phenotype of the VMAT1- and VMAT2-positive pancreatic cell populations by confocal laser scanning microscopy and dual-color IHC. The expression profiles of VMAT1 and VMAT2 in the normal endocrine pancreas were used to determine whether VMAT1- and VMAT2-positive cell lineages could be distinguished in a large series of infants with hyperinsulinemic hypoglycemia and in pancreatic endocrine tumors in adults.

Materials and Methods

Origin of Tissues

Samples of non-neoplastic human pancreas were collected during abdominal surgery from patients suffering from pancreatic adenocarcinoma (two men and two women; mean age 64 years, range 58–79; classical Whipple resection in two cases and pancreatic tail resection in two cases). Pancreatic specimens were also obtained from five rhesus monkeys (Rausch et al. 1994). The specificity and sensitivity of the

VMAT1 and VMAT2 antibodies and the VMAT1 and VMAT2 antisense probes were tested in various human and monkey tissues, including adrenal medulla, stomach, small intestine, one gastric ECL cell tumor, and two intestinal EC cell tumors.

Further non-neoplastic samples were obtained from the pancreas of 11 children with hyperinsulinemic hypoglycemia of infancy showing focal ($n=2$) or diffuse ($n=9$) β-cell hyperplasia. All children suffered from recurrent hypoglycemia and revealed high serum insulin levels.

Tumor tissue was obtained from 92 patients. All tumors were classified according to the WHO criteria (Solcia et al. 2000) including size, cell differentiation, angioinvasion, proliferation index, metastatic spread, hormone expression, and functional activity. PETs were classified as well-differentiated neuroendocrine tumors (NETs), well-differentiated neuroendocrine carcinomas (NECs), and poorly differentiated NECs.

A total of 61 of 92 patients with PETs had elevated serum levels of the respective hormones and exhibited specific clinical syndromes [insulinoma ($n=44$), gastrinoma ($n=11$), EC cell tumors ($n=2$), VIPoma ($n=1$), ACTH-secreting tumors ($n=2$), and one poorly differentiated NEC with paraneoplastic hypercalcemia]. A total of 31 PETs were functionally inactive; they included five well-differentiated NETs, 22 well-differentiated NECs, and four poorly differentiated NECs.

Tissue Preparation

For IHC analysis the human tissues were fixed in either Bouin–Hollande fixative, 10% formalin, or 4% formaldehyde/PBS for 48 hr and then embedded in paraffin. The monkey tissues were perfused with 4% formaldehyde/PBS before postfixation in Bouin–Hollande for 24–48 hrs as described previously (Rausch et al. 1994).

After dehydration in a graded series of 2-propanol solutions, the tissues were embedded in Paraplast Plus (Merck; Darmstadt, Germany). Adjacent sections (3-µm or 7-µm thick) were cut and deparaffinized. Antigen retrieval to increase the sensitivity of immunodetection was performed by heating the sections at 92–95C for 15 min in 0.01 M citrate buffer (pH 6) according to the DAKO protocol (Hamburg, Germany). Nonspecific binding sites were blocked with 5% bovine serum albumin (BSA; Serva, Heidelberg, Germany) in PBS, followed by an avidin–biotin blocking step (avidin–biotin blocking kit; Boehringer, Ingelheim, Germany).

For ISH, human non-neoplastic pancreatic tissues and 11 endocrine tumors were immediately frozen on dry ice and stored at −80C. Cryosections (14–16-µm thick) were placed on pre-silanized glass slides, fixed in 4% phosphate-buffered formaldehyde for 60 min, followed by three 10 min washes in 50 mM PBS (pH 7.4). The slides were then briefly rinsed in distilled water, incubated in 0.1 M triethanolamine (pH 8.0) for 1 min, and for 10 min in the same solution containing 0.25% v/v acetic anhydride under rapid stirring. They were then quickly rinsed in 2 × SSC, dehydrated in 50 and 70% ethanol, and air-dried.

Immunohistochemistry

Rabbit antiserum no. VMAT1/10 raised against the C-terminal sequence of human VMAT1 and antiserum no. 80182

raised against the C-terminal sequence of human VMAT2 were employed for the immunohistochemical investigations (Table 1). Several antisera against general neuroendocrine markers, serotonin, and various peptide hormones were used (Table 1).

Tissue sections were incubated with the primary antibodies overnight at 18C (diluted as shown in Table 1) and further incubated for 2 hr at 37C. After washing in distilled water and in 50 mM PBS, sections were incubated with species-specific biotinylated secondary antibodies (Dianova; Hamburg, Germany) for 45 min at 37C, washed several times, and incubated for 30 min with the ABC reagents (Vectastatin Elite ABC kit; Boehringer). Immunoreactions were visualized with 3′3-diaminobenzidine (DAB; Sigma, Deisenhofen, Germany) enhanced by the addition of 0.08% ammonium nickel sulfate (Fluka; Buchs, Switzerland), resulting in dark blue staining. No binding was detected in the absence of the primary antibody. The specificity of the IHC staining was demonstrated by preabsorbing the antisera with 25 μmol of the C-terminal human VMAT1 and VMAT2 peptide, respectively. VMAT1 and VMAT2 were detectable in tissues fixed either in Bouin–Hollande or in 4% (para)formaldehyde with or without antigen retrieval.

The number of VMAT1- and VMAT2-positive cells in neuroendocrine tumors was estimated semiquantitatively as approximate percentage and scored on a scale from − (absent), (+) (extremely sparse), + (< 10%), ++ (10–<20%), +++ (20–<40%), ++++ (40–<60%) to +++++ (60–100%).

In Situ Hybridization

To generate specific probes for the localization of VMAT1 mRNA, a 247-bp-long DNA restriction fragment of the hVMAT1 cDNA (Erickson et al. 1996) corresponding to nt. 436–682 was subcloned into Bluescript II KS+ (Stratagene; Heidelberg, Germany). For VMAT2 mRNA detection, a 269-bp-long DNA fragment of the hVMAT2 cDNA (Erickson and Eiden 1993) corresponding to nt. 244–512 was subcloned into pcDNAI (Invitrogen; Leek, Netherlands). Inserted sequences were verified by double-stranded DNA sequencing. In vitro transcription of the two vector constructs using [^{35}S]-UTP-labeled nucleotide yielded antisense riboprobes for hVMAT1 after linearization with XhoI and incubation with T7 RNA polymerase, and for hVMAT2 after linearization with XbaI and incubation with SP6 RNA polymerase. To increase the tissue penetration of probes, generated transcripts were reduced to about 200 nt. fragments by limited alkaline hydrolysis, as described by Angerer et al. (1987).

To each section hybridization buffer (3 × SSC, 50 mM NaPO$_4$, pH 7.4, 1 × Denhardt's solution, 0.25 mg/ml yeast tRNA, 10% dextran sulfate, 50% formamide, 10 mM dithiothreitol) was applied. The hybridization mix contained 50,000 dpm/ml of ^{35}S-labeled RNA probes. Sections were coverslipped and incubated in moist chambers at 60C for 16 hr. The coverslips were then removed in 2 × SSC. The sections were then subjected to the following posthybridization steps: RNAse treatment (20 μg/ml RNase A and 1 U/ml

Table 1 List of primary antibodies

Antigen	Code	Source/Reference	Dilution	Species
VMAT1	VMAT1/10	Erickson et al. 1996	1:4000/1:300 (f)[a]	Rabbit, polyclonal
VMAT2	80182	Erickson et al. 1996	1:4000/1:400 (f)	Rabbit, polyclonal
Serotonin	5-HT H209	DAKO; Hamburg, Germany	1:20/1:2 (f)	Mouse, monoclonal
Serotonin	5-HT 43H37R	INC/IBL, Hamburg, Germany	1:60,000/1:4000 (f)	Rabbit, polyclonal
Serotonin	B56-1	Euro-Diagnostica, Germany	1:50	Rabbit, polyclonal
Chromogranin A	WE-14 Lenny 9	Hörsch et al. 1993	1:10,000	Rabbit, polyclonal
Chromogranin A	LK2H10	Boehringer; Mannheim, Germany	1:200/1:20 (f)	Mouse, monoclonal
Synaptophysin	A0010	DAKO	1:50	Rabbit, polyclonal
Synaptophysin	M0776	DAKO	1:15	Mouse, monoclonal
ACTH[b]	M3501	DAKO	1:500	Mouse, monoclonal
Gastrin	A568	DAKO	1:30,000/1:2000 (f)	Rabbit, polyclonal
Gastrin	AC7A1	Immunotech, Marseille, France	1:500/1:40 (f)	Mouse, monoclonal
Glucagon	A0565	DAKO	1:6000	Rabbit, polyclonal
Glucagon	039P	BioGenex, San Ramon, CA	1:60	Rabbit, polyclonal
Glucagon	SC-7780	Santa Cruz Technology, Santa Cruz, CA	1:600 (f)	Goat, polyclonal
Insulin	045A	DAKO	1:6000/1:600 (f)	Guinea pig, monoclonal
Insulin	029M	BioGenex, San Ramon, CA	1:40	Mouse, monoclonal
Pancreatic polypeptide	95095318	Pasel and Lorey, Germany	1:6000	Rabbit, polyclonal
Pancreatic polypeptide	PH512	The Binding Site, Birmingham, UK	1:60 (f)	Sheep, polyclonal
Somatostatin	PEPA 38	Serotec, Oxford, UK	1:8000	Rabbit, polyclonal
Somatostatin	A0566	DAKO	1:200	Rabbit, polyclonal
Somatostatin	BM715	Biermann, Bad Nauheim, Germany	1:40 (f)	Rat, monoclonal
VIP[c]	18-0080	Zymed, San Francisco, CA	1:10	Rabbit, polyclonal
VIP	VIP-Y010	Yanaihara, Shizuoka, Japan	1:10,000/1:1000 (f)	Rabbit polyclonal

[a]Dilution for immunofluorescence.
[b]Adrenocorticotrophic hormone.
[c]Vasoactive intestinal peptide.

RNase T1 in 10 mM Tris, pH 8.0, 0.5 M NaCl, 1 mM EDTA) for 60 min at 37C and successive washes in decreasing salt concentrations (2 $\times$, 1 $\times$, 0.5 $\times$, and 0.2 $\times$ SSC) for 10 min each, followed by incubation in 0.2 $\times$ SSC at 60C for 60 min. For autoradiography, slides were dipped in NTB-2 nuclear emulsion (Eastman Kodak; Rochester, NY) and developed after 3 weeks of exposure time. Developed sections were stained with hematoxylin and eosin, analyzed, and photographed in darkfield and brightfield modes with an Olympus AX 70 microscope (Hamburg, Germany).

Co-localization Studies

To study the co-localization of VMAT1 and VMAT2 with the respective neuroendocrine markers, three strategies were used: (a) alternate staining of adjacent semithin sections (2–3 μm thick), (b) the two-color immunoperoxidase technique (Hancock 1986), and (c) double-fluorescence labeling (Hörsch et al. 1993). The cellular distribution of antigens visualized by double fluorescence was analyzed by confocal laser scanning microscopy.

For adjacent section analysis, randomly selected pairs of semithin sections were stained for each marker combination as described above. For the two-color peroxidase technique, the first primary antibody was detected with the nickel-enhanced DAB procedure. After dehydration through a graded series of 2-propanol and one passage through xylene, the sections were rehydrated in a graded series of 2-propanol and treated with BSA and the avidin–biotin reagents to block potential nonspecific binding of the second avidin–biotin–peroxidase complex. The second primary antibody was then visualized by DAB/peroxidase reaction without nickel enhancement, resulting in a brown staining product. In control sections, the primary antibodies were omitted.

Double immunofluorescence detection was performed by covering the sections with a mixture of the two different primary antibodies in appropriate dilutions (Table 1) and by subsequent labeling with the species-specific secondary antibodies bearing the Alexa fluorochromes A647, A594, or A488 (MoBiTec; Göttingen, Germany) or the fluochromes Cy2 or Cy3 (Dianova; Hamburg, Germany). Furthermore, streptavidin coupled with Alexa fluochromes A647, A488, or A594 (MoBiTec) or with Cy2 or Cy3 was used in combination with biotinylated species-specific secondary antisera bearing the appropriate fluochrome. For conventional double immunofluorescence, sections were analyzed and photographed with an AX 70 microscope (Olympus) equipped with the appropriate filter cubes for discriminating among the different fluochromes). Confocal double immunofluorescence analysis was performed with the Fluoview laser scanning microscope (Olympus). Digital confocal images were presented in false color.

Ethics

Results

Mutually Exclusive Expression of VMAT2 in β-cells and VMAT1 in EC Cells of the Primate Pancreas

In all regions of the human and monkey pancreas examined in this study, VMAT2 was present in a considerable subpopulation of pancreatic islet cells, as demonstrated by IHC and ISH (Figures 1 and 2). VMAT2 was also detectable in varicose nerve fibers innervating the pancreatic islets, intra- and interlobular ducts, the exocrine parenchyma, and blood vessels (Figure 1). In contrast, islet cells did not reveal any positivity for VMAT1 and serotonin (data not shown). ISH revealed specific strong signals for VMAT2 in the ma-
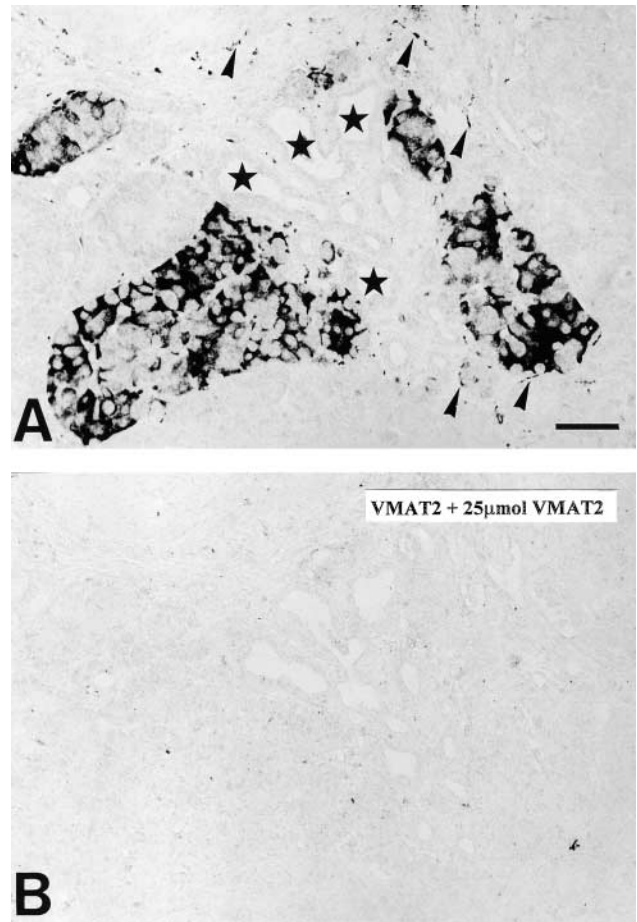

Figure 1 Immunohistochemistry for VMAT2 in human pancreas. **(A)** Low-power magnification revealing VMAT2 expression in a considerable subpopulation of neuroendocrine cells of four islets of Langerhans. VMAT2 is absent from small intralobular pancreatic ducts (asterisk) and epithelial cells of the exocrine parenchyma. The exocrine parenchyma and the periphery of islets are innervated by sparsely distributed VMAT2-positive nerve fibers (arrowheads). **(B)** VMAT2 immunostaining of neuroendocrine cells and nerve fibers is abolished in an adjacent section after preincubation of the VMAT2 antiserum with 25 μmol VMAT2 peptide. Bar = 50 μm.
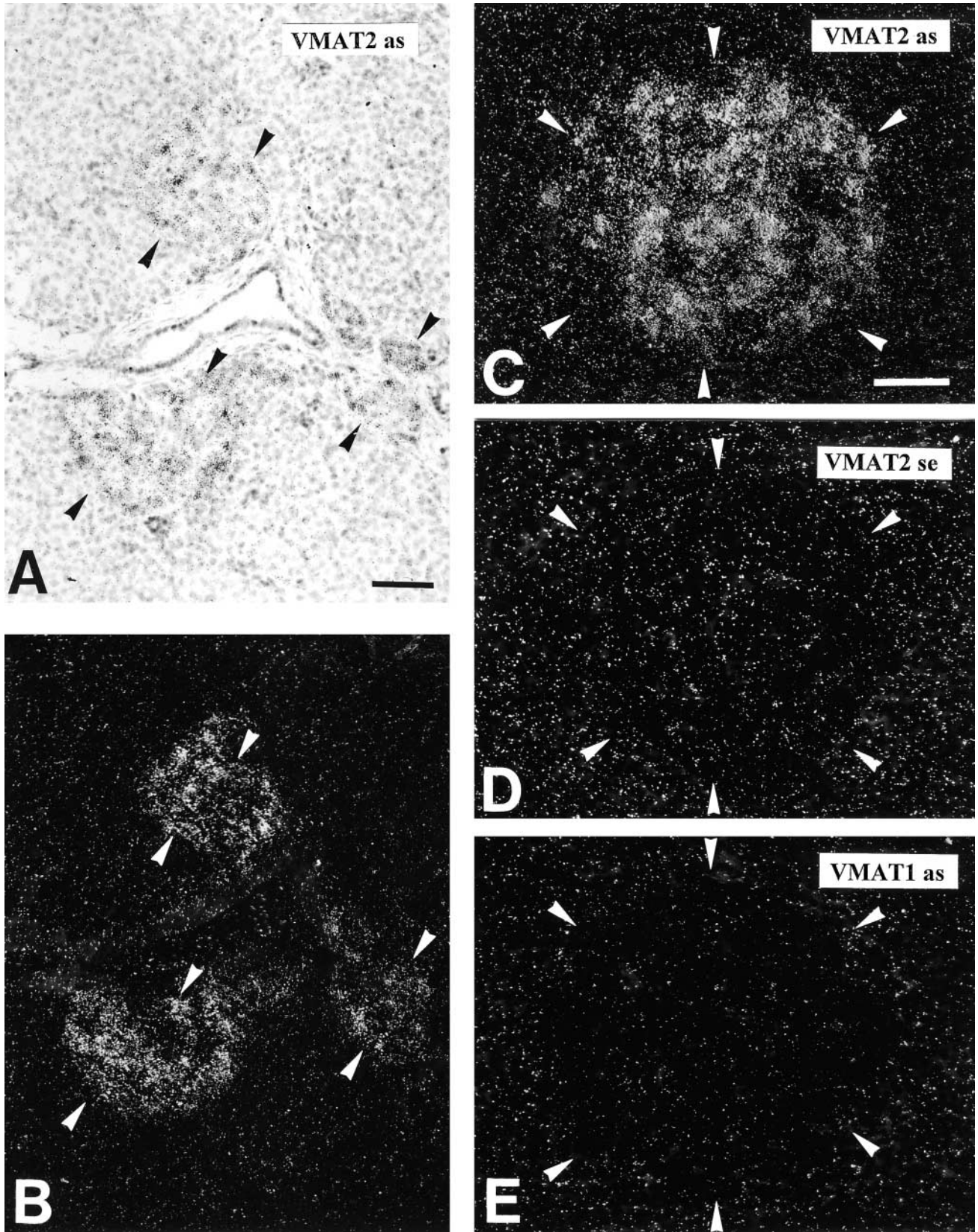
Figure 2 Comparison of VMAT1 and VMAT2 mRNA expression in the human pancreas. **(A,B)** Low-power magnification of an identical section photographed in brightfield **(A)** and darkfield **(B)** illumination. Hybridization with a VMAT2 antisense cRNA probe (VMAT2 as) reveals a selective signal in the majority of neuroendocrine cells of three islets (arrowheads). **(C–E)** High-power darkfield magnification of an islet on adjacent sections. The boundary of the islet is labeled by arrowheads in **C–E**. After hybridization with a VMAT2 antisense cRNA probe, many endocrine cells of the islet but no exocrine cells are positively labeled **(C)**. Hybridization with a VMAT2 probe in sense strand orientation (VMAT2 se) yields only background labeling **(D)**. No hybridization signal was seen for the VMAT1 antisense cRNA probe (VMAT1 as). Exposure times of emulsion-coated slides were 21 days. Bars: **A,B** = 50 μm; **C–E** = 50 μm.
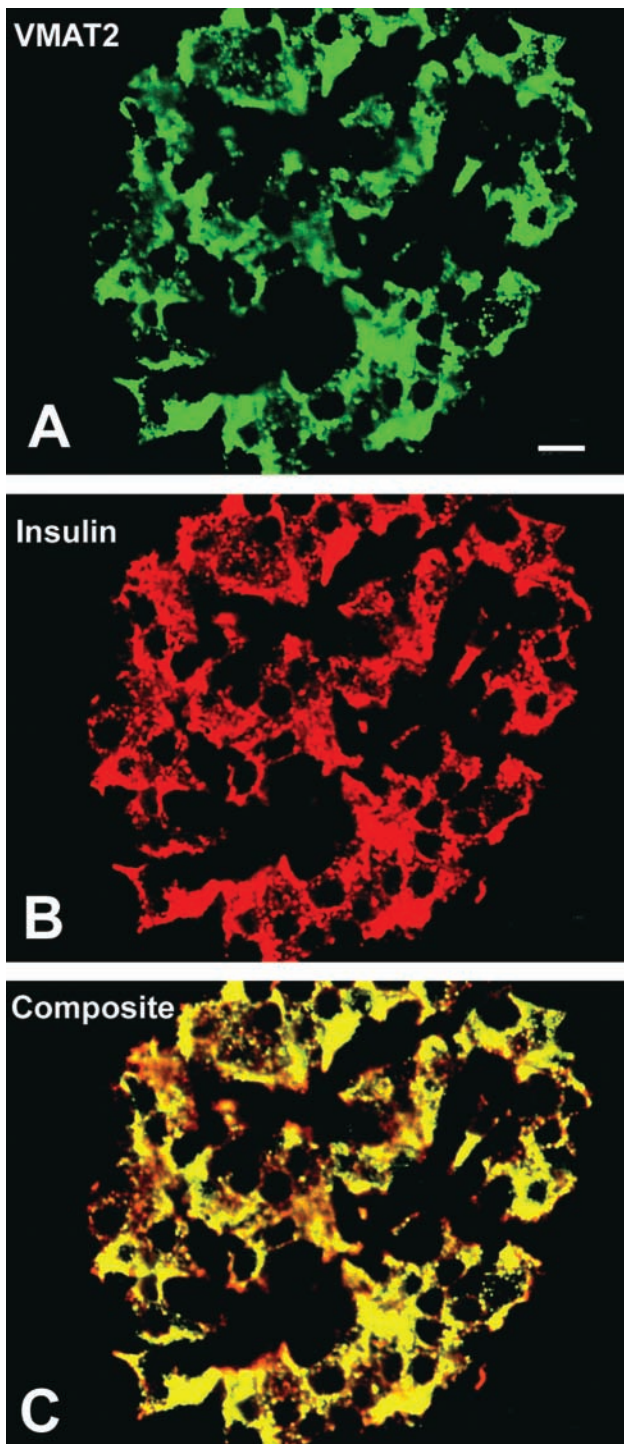
Figure 3 Identification of the cellular phenotype of VMAT2-immunoreactive cells in human pancreatic islets by confocal laser scanning microscopy. **(A–C)** High-resolution confocal laser microscopy in an identical section through a pancreatic islet showing a similar distribution pattern of cells positive for VMAT2 **(A)** and insulin **(B)**. The yellow color in the composite image **(C)** indicates cellular co-localization of the two antigens. Bars = 10 μm.

jority of islet cells (Figure 2). In contrast, VMAT1 mRNA was lacking from pancreatic islets (Figure 2).

Confocal laser scanning microscopy demonstrated the presence of VMAT2 in insulin-immunoreactive cells (Figure 3). In contrast, VMAT2 was strictly absent from glucagon, somatostatin, and pancreatic polypeptide cells, as shown by the analysis of semithin adjacent sections, dual-color IHC, and confocal laser scanning microscopy (Figure 4). This observation was also confirmed in all cases of infants with hyperinsulinemic hypoglycemia. In diffuse or focal β-cell hyperplasia all β-cells expressed exclusively VMAT2 but not VMAT1 (data not shown). VMAT1 was exclusively present in cells of the intra- and interlobular duct system in the pancreas. All VMAT1-immunoreactive cells were co-positive for serotonin and CgA (Figure 5), but negative for insulin, glucagon, somatostatin, and pancreatic polypeptide.

The specificity and sensitivity of the VMAT1 antibody and the VMAT1 antisense probe were tested in various human and monkey tissues. VMAT1 protein and mRNA were easily visualized in these control tissues (data not shown). Neither VMAT1 nor VMAT2 immunoreactivity nor mRNA was expressed in pancreatic exocrine cells.

Loss of VMAT2 in Many Insulinomas, Expression of VMAT2 in Tumors Other than Insulinomas, and Conservation of VMAT1 in EC Cell Tumors

A minor proportion of insulinomas revealed expression of VMAT2, as demonstrated by IHC and ISH. VMAT2-positive cells were detected in 10 of 34 benign insulinomas and 5 of 10 malignant insulinomas (Figure 6; and Table 2). The VMAT2-positive cells were present in subpopulations of insulin-positive tumor cells and were distributed either diffusely or focally (Figure 7; and Table 2).

Some non-insulinomas revealed expression of VMAT2 in subpopulations of tumor cells. These consisted of two of 11 gastrinomas, one EC cell tumor, one ACTH-producing tumor, and eight of 31 nonfunctioning pancreatic neuroendocrine tumors (Tables 3 and 4). All beta cells in islets adjacent to the neuroendocrine tumors showed positivity for VMAT2 (Tables 2–4).

VMAT1 was absent from all but three PETs, which were found to express serotonin (Tables 2–4).

Discussion

The monoamine-containing neuroendocrine cell system is characterized by the expression of VMAT1 or VMAT2, which mediate monoamine uptake into secretory granules (Weihe and Eiden 2000; Eiden et al. 2002). In this study we demonstrated that in the normal endocrine pancreas only EC (serotonin-containing) cells express VMAT1 and only β-cells express

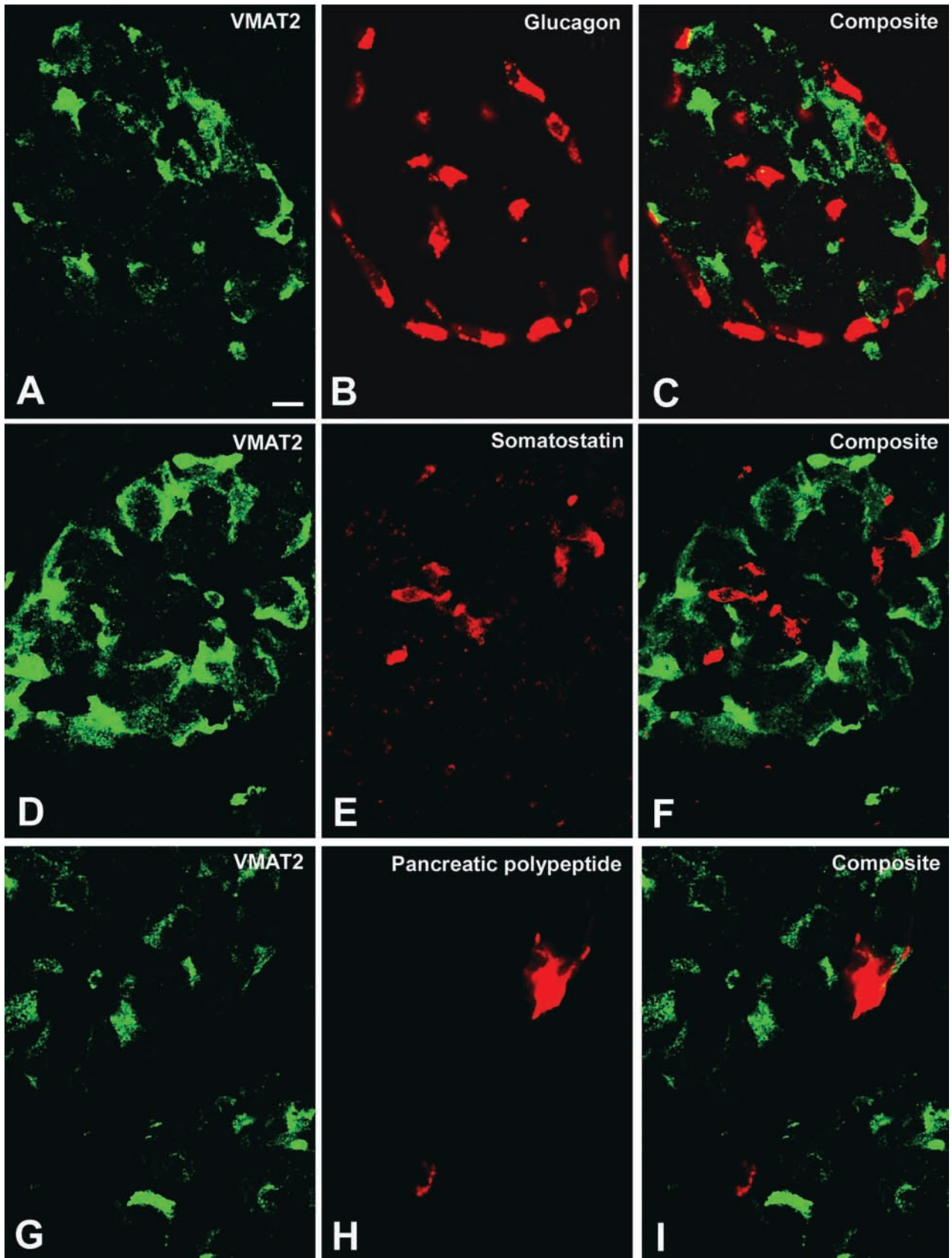**Figure 4** Absence of VMAT2 from glucagon, somatostatin, and pancreatic polypeptide cells demonstrated by confocal laser scanning microscopy. (**A–I**) High-resolution confocal laser microscopy through pancreatic islets revealing strict segregation of VMAT2 and glucagon (**A–C**), VMAT2 and somatostatin (**D–F**), and VMAT 2 and pancreatic polypeptide (**G–I**). Bars = 20 μm.
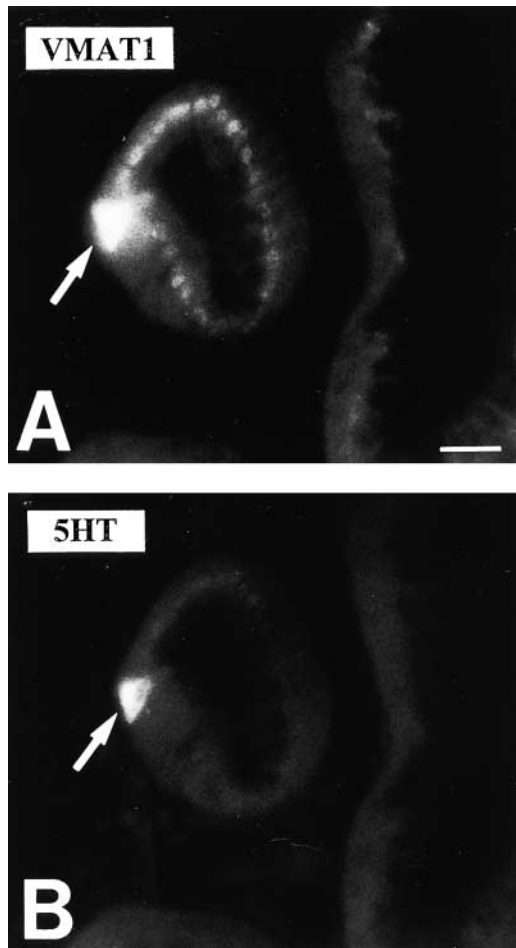
Figure 5 Identification of the cellular phenotype of VMAT1-immunoreactive cells in the rhesus monkey pancreatic duct system by double fluorescence analysis. **(A,B)** VMAT1 **(A)** is coexistent with serotonin (5HT) **(B)** in neuroendocrine cells of small pancreatic intralobular ducts. Bar = 10 μm.

VMAT2. Neoplastic beta cells (i.e. insulinoma cells), however, partially lose the feature of VMAT2 expression, while neoplastic EC cells (i.e. the cells of serotonin-containing tumors) retain the capacity to express VMAT1.

Normal Pancreas and Hyperinsulemic Hypoglycemia of Infancy (Nesidioblastosis)

We demonstrated the exclusive expression of VMAT2 in normal beta cells in both humans and monkeys. The expression of VMAT2 in beta cells did not appear to be changed by hyperfunction, since the beta cells of children with hyperinsulinemic hypoglycemia of infancy showed the same expression pattern.

Vesicular monoamine transporters are responsible for the uptake of biogenic amine into secretory gran-

ules to make it available for exocytotic release (Erickson et al. 1996; Eiden 2000). The selective expression of VMAT2 in beta cells adds a new important feature to the functional spectrum of this particular cell type. Expression of VMAT2 is an indication of vesicular accumulation of monoamines, which are most likely released together with insulin from beta-cells. The physiological action of monoamines such as histamine, norepinephrine, dopamine and serotonin on the secretion of islet hormones is well documented (Lindstrom and Sehlin 1983; Ahren and Lundquist 1985; Jones et al. 1987; Sener et al. 1990; Persaud et al. 1993; Cable et al. 1995; Sjoholm 1995; Coulie et al. 1998; Yajima et al. 2001). Previous studies on the presence of monoamines, monoamine-synthesizing enzymes, and monoamine uptake in the islets of the non-primate pancreas (rat, mouse, hamster, and guinea pig) using various histochemical and chemical methods have yielded widely differing results (Mahony and Feldman 1977; Ahren and Lundquist 1985; Lundquist et al. 1989; Cetin 1992; Iturriza and Thibault 1993; Teitelman et al. 1993; Furuzawa et al. 1994; Barbosa et al. 1998). The specific phenotype and function of the monoamine(s) in normal primate β-cells remain to be identified. Our own observations in mouse, rat, and dog suggest marked species and developmental differences in the cell type-specificity of VMAT1 and VMAT2 expression in pancreatic islets, which fundamentally differ from human and rhesus monkey (Anlauf and Weihe, unpublished observations; and this study) and need to be fully explored in future studies. This underlines the unique situation in primates documented in the present study in which VMAT2 was found to be expressed in insulin-secreting β-cells but not in glucagon, somatostatin, and pancreatic polypeptide cells.

VMAT1 has been established as a marker of the normal EC cell in the gut (Weihe et al. 1994; Erickson et al. 1996). Scattered VMAT1-positive cells were previously observed in pancreatic islets closely associated with endocrine tumor tissue (Jakobsen et al. 2001). However, in our investigation of the normal primate endocrine pancreas, VMAT1-immunoreactive and VMAT1 mRNA-expressing cells were detected only in cells of the inter- and intralobular ducts, and not in or surrounding pancreatic islets themselves or in individual hormone-secreting cells found throughout the exocrine pancreas. The VMAT1-positive cells of the pancreas are neuroendocrine cells, based on their chromogranin A-positive phenotype. Double-fluorescence analysis revealed that these VMAT1-positive duct-associated cells contain serotonin. Their distribution corresponded to serotonin-producing cells described by others in the pancreatic ducts (Carlei et al. 1993). Regarding the function of VMAT1, it is of interest that recent studies in the guinea pig and rat indi-
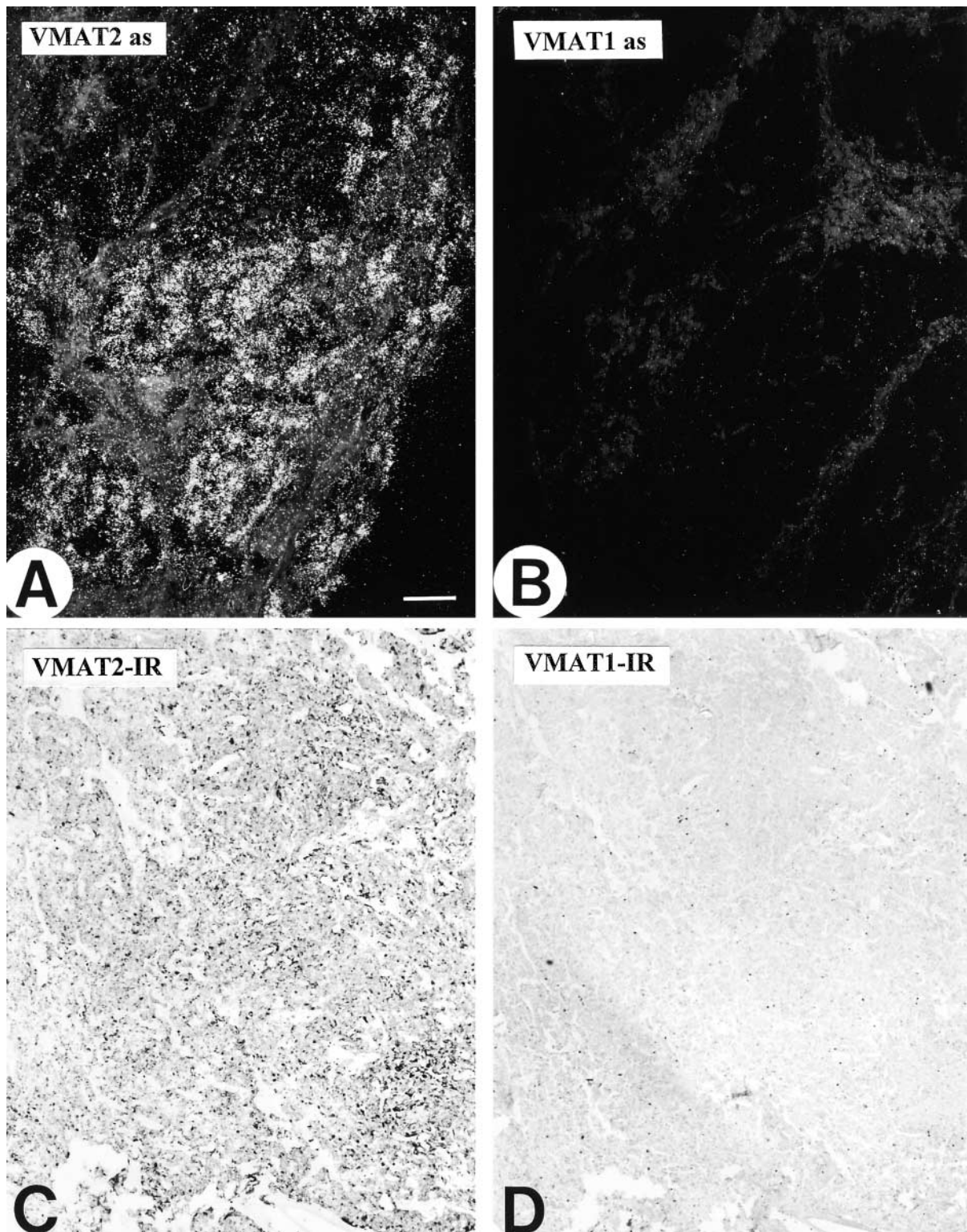
Figure 6 Distribution of VMAT1 and VMAT2 in an insulinoma investigated by IHC and ISH. **(A–D)** Diffuse distribution pattern of VMAT2 mRNA **(A)** and VMAT2 protein **(C)** in a well-differentiated insulin-secreting NEC (no. 13 in Table 2). In contrast, VMAT1 mRNA **(B)** and VMAT1 protein **(D)** are lacking in this insulinoma **(B,D)**. Bar = 200 μm.

Table 2　Expression of VMAT1 and VMAT2 in insulin-secreting benign and malignant insulinomas

No./Init.[a]	VMAT1	VMAT2	Size (cm)	Angioinv.[b]	Metast.[c]	Classification
1 B.C.	−	+++++	1.2 × 0.7	No	No	Well-differentiated NET
2 M.J.	−	−	1.4 × 1.0	No	No	Well-differentiated NET[f]
3 W.H.	−	−	1.1 × 0.7	No	No	Well-differentiated NET
4 K.K.	−	−	1.5 × 1.0	No	No	Well-differentiated NET[f]
5 W.H.	−	−	1.5 × 0.9	Yes	No	Well-differentiated NET[f]
6 R.D.	−	−	0.8 × 0.7	No	No	Well-differentiated NET
7 Z.E.	−	−	1.8 × 1.4	No	No	Well-differentiated NET
8 M.J.	−	−	1.4 × 1.0	No	No	Well-differentiated NET[f]
9 K.K.	−	−	1.5 × 1.0	No	No	Well-differentiated NET[f]
10 M.K.	−	−	1.4 × 1.2	No	No	Well-differentiated NET
11 R.H.	−	+	1.5 × 1.5	No	No	Well-differentiated NET
12 K.H.	−	−	1.0 × 1.0	No	No	Well-differentiated NET[f]
13 F.K.	−	+++	1.0 × 1.0	No	No	Well-differentiated NET
14 n.k.[d]	−	+	1.3 × 1.0(m)[e]	No	No	Well-differentiated NET[f]
15 D.C.	−	−	0.5 × 0.3(m)	No	No	Well-differentiated NET
16 W.H.	−	−	1.5 × 1.0	No	No	Well-differentiated NET
17 W.K.	−	−	1.0 × 0.8	No	No	Well-differentiated NET
18 D.L.	−	−	1.2 × 1.0	No	No	Well-differentiated NET
19 H.B.	−	−	1.2 × 1.0	No	No	Well-differentiated NET[f]
20 M.V.	−	−	1.5 × 1.5	No	No	Well-differentiated NET[f]
21 G.F.	−	++++	1.0 × 1.0	No	No	Well-differentiated NET
22 D.M.	−	++	1.5 × 1.2	No	No	Well-differentiated NET[f]
23 F.S.	−	−	1.8 × 1.0	No	No	Well-differentiated NET
24 Z.B.	−	−	< 0.5(m)	No	No	Well-differentiated NET
25 E.M.	−	−	1.1 × 0.8	No	No	Well-differentiated NET[f]
26 R.R.	−	−	1.5 × 1.5(m)	No	No	Well-differentiated NET[f]
27 M.H.	−	−	2.0 × 1.5	No	No	Well-differentiated NET[f]
28 B.M.	−	++	< 1.0	No	No	Well-differentiated NET[f]
29 S.R.	−	−	0.8 × 0.5	No	No	Well-differentiated NET[f]
30 K.R.	−	−	1.2 × 0.8	No	No	Well-differentiated NET
31 B.D.	−	−	1.5 × 1.0	No	No	Well-differentiated NET
32 A.I.	−	++++	< 0.8	No	No	Well-differentiated NET[f]
33 R.K.	−	+	n.k.	No	No	Well-differentiated NET
34 S.I.	−	+	1.5 × 1.0	No	No	Well-differentiated NET[f]
35 D.M.	−	++++	4.5 × 2.3	Yes	Yes	Well-differentiated NEC[f]
36 S.W.	−	−	4.1 × 3.7	Yes	Yes	Well-differentiated NEC[f]
37 R.E.	−	++++	3.5 × 2.8	Yes	n.k.	Well-differentiated NEC
38 B.E.	−	−	8.0 × 6.0	Yes	Yes	Well-differentiated NEC
39 K.H.	−	++++	2.5 × 2.0	Yes	n.k.	Well-differentiated NEC
40 B.F.	−	−	3.0 × 2.0	Yes	Yes	Well-differentiated NEC
41 SW	−	+	8.0 × 7.0	Yes	Yes	Well-differentiated NEC
42 H.M.	−	−	11 × 7	Yes	Yes	Well-differentiated NEC
43 HM	−	−	2 × 1.5	Yes	Yes	Well-differentiated NEC[f]
44 S.V.	−	+	4 × 3	Yes	Yes	Well-differentiated NEC

[a]Number and initials.
[b]Angioinvasion.
[c]Metastases.
[d]Not known.
[e]Occurrence of multiple endocrine tumors.
[f]Presence of normal pancreatic islets in close association with the endocrine tumor tissue.

cate that serotonin-positive cells in the pancreatic ducts most likely mediate the fluid secretion of duct cells expressing serotonin receptors (Masuda et al. 1997; Li et al. 2000; Suzuki et al. 2001).

Pancreatic Endocrine Tumors (PETs)

Based on the mutually exclusive expression of VMAT1 in EC cells within the pancreatic duct system and of VMAT2 in the β-cells of the islets of Langerhans, we anticipated that VMAT1 and VMAT2 might also serve as markers for the neoplastic counterparts of these cells in the neuroendocrine tumors of the pancreas. This is indeed the case for VMAT1, which labeled only the three serotonin-positive neoplasms in our series of 92 different PETs, including all relevant types belonging to this tumor group. We can
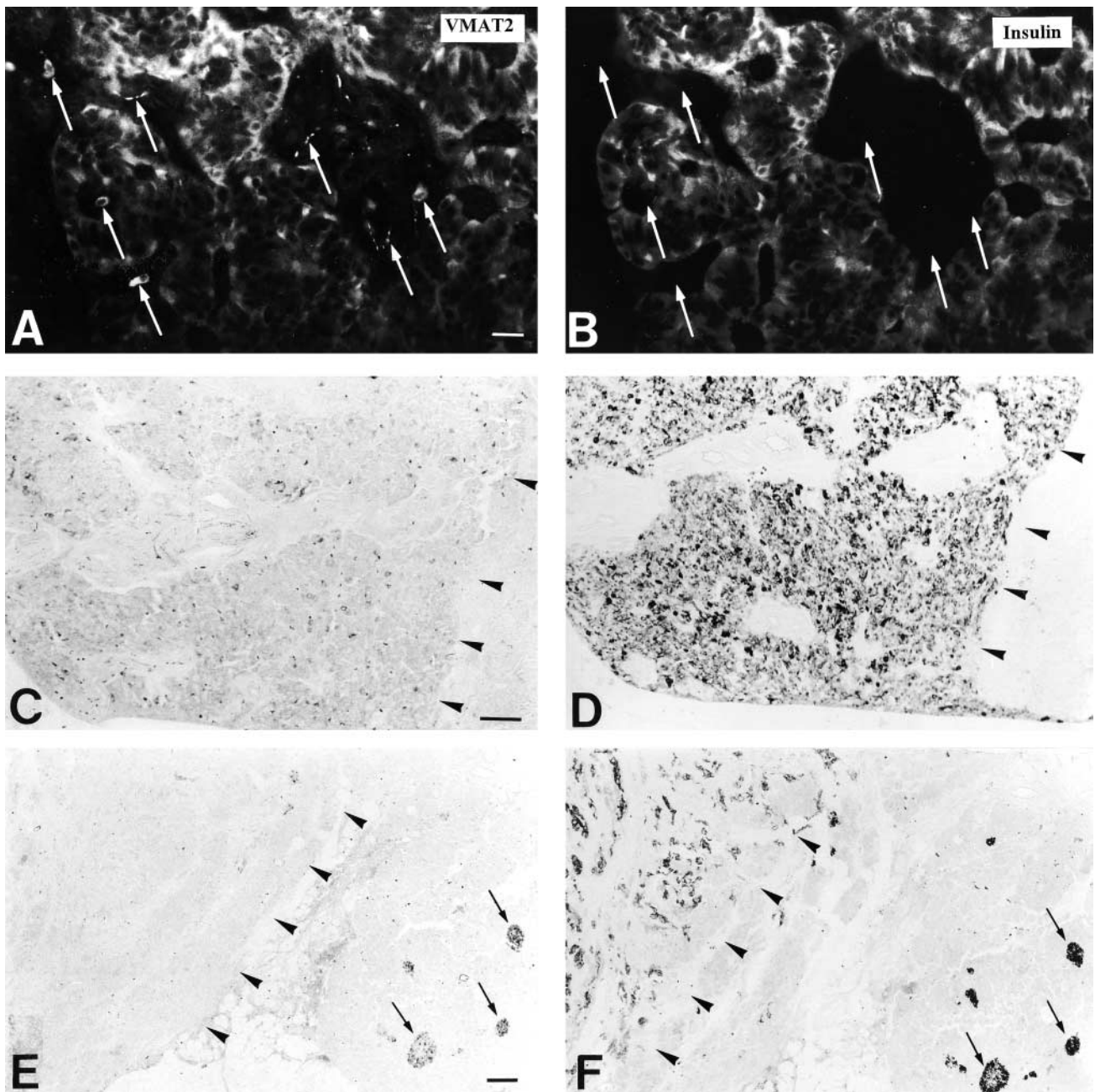
Figure 7 Differential expression of VMAT2 in three different types of insulinomas investigated by IHC. **(A,B)** Double fluorescence analysis showing full overlap of VMAT2 and insulin immunoreactivity in neuroendocrine tumor cells (no. 1 in Table 2). Note the absence of insulin from some VMAT2-positive nerve fibers and connective tissue mast cells labeled by arrows. **(C,D)** Adjacent section analysis of insulinoma no. 11 (Table 2) demonstrating expression of VMAT2 in a minor population of insulin-positive tumor cells. **(E,F)** Adjacent section analysis of an insulinoma showing the disparity between the absence of VMAT2 from insulinoma tissue and the simultaneous presence of VMAT2 in three paratumorous islets (no. 2 in Table 2). The boundaries of the neuroendocrine tumors are labeled by arrowheads **(C–F)**. Bars: **A,B** = 20 μm; **C,D** = 100 μm; **E,F** = 150 μm.

therefore extend the marker function of VMAT1 from EC cell tumors of the gut (Eissele et al. 1999) to the same tumor type in the pancreas. Concerning VMAT2, it has been reported that it occurs not only in insulinomas, but also in other functioning and nonfunctioning PETs (Rindi et al. 2000; Jakobsen et al. 2001). We extend this observation by showing that approximately one third of insulinomas express VMAT2, whether they are benign or malignant.

Table 3 Expression of VMAT1 and VMAT2 in functionally active pancreatic endocrine tumors other than insulinomas

No./Init.	VMAT1	VMAT2	Size (cm)	Angioinv.	Metast.	Immunoph.[a]	Clinical syndrome	Classification
45 T.J.F.	−	−	2.1 × 1.5	Yes	Yes	Gastrinoma	Zollinger–Ellison syndrome	Well-differentiated NET[c]
46 M.H.T.	−	−	1.1 × 0.6	No	No	Gastrinoma	Zollinger–Ellison syndrome	Well-differentiated NET[c]
47 B.O.	−	−	3.2 × 2.8	Yes	Yes	Gastrinoma	Zollinger–Ellison syndrome	Well-differentiated NEC[c]
48 A.F.	−	−	2.0 × 1.7	Yes	n.k.	Gastrinoma	Zollinger–Ellison syndrome	Well-differentiated NEC
49 A.F.	−	−	2.0 × 1.7	Yes	n.k.	Gastrinoma	Zollinger–Ellison syndrome	Well-differentiated NEC
50 E.F.	−	−	1.4 × 1.1	Yes	n.k.	Gastrinoma	Zollinger–Ellison syndrome	Well-differentiated NEC[c]
51 F.L.	−	−	5.0 × 4.5	Yes	Yes	Gastrinoma	Zollinger–Ellison syndrome	Well-differentiated NEC
52 KW	−	−	3.0 × 2.5	Yes	Yes	Gastrinoma	Zollinger–Ellison syndrome	Well-differentiated NEC
53 G.E.	−	+++	3.5 × 3.0	Yes	Yes	Gastrinoma	Zollinger–Ellison syndrome	Well-differentiated NEC
54 P.L.	−	++	9.0 × 6.0	Yes	Yes	Gastrinoma	Zollinger–Ellison syndrome	Well-differentiated NEC[c]
55 J.D.	−	−	3.8 × 3.0	Yes	Yes	Gastrinoma	Zollinger–Ellison syndrome	Well-differentiated NEC[c]
56 T.W.	+++++	+	1.5 × 0.7	Yes	n.k.	EC cell tumor	Carcinoid syndrome	Well-differentiated NEC
57 R.I.	++++	−	2.5 × 1.5	Yes	Yes	EC cell tumor	Carcinoid syndrome	Well-differentiated NEC
58 K.M.	−	++++	2.3 × 2.0	Yes	Yes	ACTHoma	Cushing syndrome	Well-differentiated NEC
59 G.R.	−	−	6.0 × 5.0	Yes	No	VIPoma	Verner–Morrison syndrome	Well-differentiated NEC
60 K.O.	−	−	n.k.	Yes	Yes	ACTHoma	Cushing syndrome	Poorly differentiated NEC
61 B.A.	−	−	5	Yes	Yes	PTH-producing tumor[b]	Paraneoplastic hypercalcemia	Poorly differentiated NEC

[a]Immunophenotype.
[b]Parathormone-producing tumor.
[c]Presence of normal pancreatic islets in close association with the endocrine tumor tissue.

Table 4 Expression of VMAT1 and VMAT2 in non-functioning pancreatic endocrine tumors

No./Init	VMAT1	VMAT2	Size (cm)	Angioinv.	Metast.	Immunoph.	Classification
62 K.A.	−	−	1.0 × 1.0	No	No	*Ins[a] ++++*	Well-differentiated NET[f]
63 N.K.	−	+	3.2 × 1.6	Yes	Yes	*Ins ++; PP[b] +; Glu[c]+*	Well-differentiated NEC
64 E.L.	−	−	3.4 × 1.8	Yes	n.k.	*Ins +*	Well-differentiated NEC
65 W.H.	−	−	3.8 × 2.7	Yes	n.k.	*Ins+; Glu+*	Well-differentiated NEC
66 B.A.	−	−	8 × 7	Yes	Yes	*Ins (+); Glu (+)*	Well-differentiated NEC
67 K.O.	−	−	<1.5	No	No	*Glu ++*	Well-differentiated NET
68 U.H.	−	−	1.5 × 0.8	No	No	*Glu +*	Well-differentiated NET
69 R.R.	−	−	3.0 × 2.5	Yes	Yes	*Glu ++*	Well-differentiated NEC
70 B.H.	−	−	3.5 × 3	Yes	Yes	*Glu +; Som[d] (+)*	Well-differentiated NEC
71 D.A.	−	++++	4 × 3	Yes	Yes	*Glu +; PP ++*	Well-differentiated NEC[f]
72 B.K.	−	+++	4.0 × 3.5	Yes	Yes	*Glu +;Som +;*	Well-differentiated NEC
73 D.E	−		2.0 × 2.0	No	No	*PP+; Som ++*	Well-differentiated NET
74 H.H.	−	++	6 × 4	Yes	Yes	*PP ++*	Well-differentiated NEC
75 S.G.	−	−	4 × 3	Yes	n.k.	*PP ++*	Well-differentiated NEC
76 H.H.	−	++	6 × 4	Yes	Yes	*PP ++*	Well-differentiated NEC
77 S.H.	−	−	6.0 × 5.0	Yes	Yes	*PP (+)*	Well-differentiated NEC
78 R.L.	−	+	2 × 2	Yes	No	*PP ++; Som+*	Well-differentiated NEC
79 S.U.	−	−	12 × 10	Yes	Yes	*PP +; Gas[e] (+)*	Well-differentiated NEC
80 V.A.	−	+	5 × 4	Yes	Yes	*Som (+)*	Well-differentiated NEC
81 B.A.	++++	−	1.3 × 0.8	No	No	*5-HT[f] ++*	Well-differentiated NET
82 S.G.	−	−	3.5 × 3.0	Yes	Yes	*No hormones*	Well-differentiated NEC
83 F.G.	−	−	7 × 5	Yes	Yes	*No hormones*	Well-differentiated NEC
84 P.I.	−	−	8 × 6	Yes	Yes	*No hormones*	Well-differentiated NEC
85 B.A.	−	−	4 × 2.5	Yes	Yes	*No hormones*	Well-differentiated NEC
86 J.K.	−	−	4.5 × 3.5	Yes	Yes	*No hormones*	Well-differentiated NEC
87 Z.D.	−	+++	4.5 × 2	Yes	Yes	*No hormones*	Well-differentiated NEC
88 S.I.	−	−	9 × 7	Yes	Yes	*No hormones*	Well-differentiated NEC
89 K.R.	−	−	n.k.	Yes	Yes	*Syn[g] +++; CgA[h] +* *Ins +; Som +; Glu+*	Poorly differentiated NEC
90 J.G.	−	−	12.5 × 10	Yes	Yes	*Syn+, CgA+; PP +*	Poorly differentiated NEC
91 G.D.	−	−	12 × 11	Yes	Yes	*CgA ++; PP ++*	Poorly differentiated NEC
92 J.M.	−	−	3.0 × 2.5	Yes	Yes	*CgA (+)*	Poorly differentiated NEC

[a]Insulin.
[b]Pancreatic polypeptide.
[c]Glucagon.
[d]Somatostatin.
[e]Gastrin.
[f]Serotonin.
[g]Synaptophysin.
[h]Chromogranin A.
[i]Presence of normal pancreatic islets in close association with the endocrine tumor tissue.

We do not yet know which additional features distinguish the two thirds of insulinomas that do not express VMAT2 from those that do express VMAT2. However, it has long been known that the presence of typical or atypical secretory granules and the abnormal conversion of proinsulin to insulin in insulinoma cells reflect the state of differentiation of the tumor cell, compared with normal β-cells (Creutzfeldt et al. 1973; Capella et al. 1977; Roth et al. 1992,1995; Azzoni et al. 1998; Komminoth et al. 1999). Electron microscopic analysis and examination of hormone processing of VMAT2-positive and VMAT2-negative insulinomas will be required to determine whether VMAT2 expression is correlated with a specific granule phenotype or abnormal prohormone processing pathways.

VMAT2 positivity in non-insulinomas was not restricted to a certain tumor type, but it occurred only in malignant tumors. However, the number of benign PETs among the non-insulinoma cases was rather small. Therefore, this finding needs to be confirmed in a larger series. PETs are frequently multihormonal. Functional and non-functional PETs may therefore contain cells that are positive for insulin, in addition to normal pancreatic cells entrapped within the tumor. We carefully screened all PETs for insulin and VMAT2. We failed to detect VMAT2 positivity even in the scattered cells of these tumors, indicating that the insulin-positive cells in neuroendocrine tumors differ from the β-cells present in the islets of Langerhans and VMAT2-positive insulinomas. There is no clear correlation between a given function of PETs and VMAT2 expression, suggesting that neither the gain nor the loss of the capability to accumulate and secrete monoamines via VMAT2 affects the functional status of neoplastic endocrine cells.

In summary, we have demonstrated the mutually exclusive expression of VMAT1 in EC cells of the duct system and of VMAT2 in β-cells of the normal primate pancreas. This expression pattern suggests that both cell types store and release monoamines. In PETs, however, only VMAT1 retains its marker function for EC cells, whereas VMAT2 can be found in both non-insulin-secreting tumors and in insulinomas. Therefore, VMA2, although not a definitive marker for determining the cell origin of pancreatic endocrine tumors, may provide a basis for diagnosis, imaging, and treatment of malignant and non-malignant non-functional PETs.

Literature Cited

Ahren B, Lundquist I (1985) Effects of L-dopa-induced dopamine accumulation on 45Ca2$^+$ efflux and insulin secretion in isolated rat islets. Pharmacology 30:71–82

Angerer LM, Stoler MH, Angerer RC (1987) In situ hybridization with RNA-probes: an annotated recipe. In Valentino L, Eberwine I, Barchas D, eds. In Situ Hybridization: Application to Neurobiology. New York, Oxford University Press, 42–70

Anlauf M, Weihe E, Hartschuh W, Hamscher G, Feurle GE (2000) Localization of xenin-immunoreactive cells in the duodenal mucosa of humans and various mammals. J Histochem Cytochem 48:1617–1626

Azzoni C, D'Adda T, Tamburrano G, Coscell C, Madsen OD, Scopsi L, Bordi (1998) Functioning human insulinomas. An immunohistochemical analysis of intracellular insulin processing. Virchows Arch 433:495–504

Barbosa RM, Silva AM, Tome AR, Stamford JA, Santos RM, Rosa LM (1998) Control of pulsatile 5-HT/insulin secretion from single mouse pancreatic islets by intracellular calcium dynamics. J Physiol 510:135–143

Cable HC, el-Mansoury A, Morgan NG (1995) Activation of alpha-2-adrenoceptors results in an increase in F-actin formation in HIT-T15 pancreatic B-cells. Biochem J 307:169–174

Capella C, Solcia E, Frigerio B, Buffa R, Usellini L, Fontana P (1977) The endocrine cells of the pancreas and related tumours. Ultrastructural study and classification. Virchows Arch [A] 373:327–352

Carlei F, Barsotti P, Crescenzi A, Bologna M, Muzi P, Schietroma M, Lomanto D, et al. (1993) Neuroendocrine epithelial cells of the main pancreatic ducts and ampulla. Ital J Gastroenterol 25:171–173

Cetin Y (1992) Biogenic amines in the guinea pig endocrine pancreas. Life Sci 50:1343–1350

Coulie B, Track J, Bouillon R, Peeters T, Janssens J (1998) 5-Hydroxytryptamine-1 receptor activation inhibits endocrine pancreatic secretion in humans. Am J Physiol 274:317–320

Creutzfeldt W, Arnold R, Creutzfeldt C, Deuticke U, Frerichs H, Track NS (1973) Biochemical and morphological investigations of 30 human insulinomas. Correlation between the tumour content of insulin and proinsulin-like components and the histological and ultrastructural appearance. Diabetologia 9:217–231

Eiden LE (2000) The vesicular neurotransmitter transporters: current perspectives and future prospects. FASEB J 14:2396–2400

Eiden LE, Schutz B, Anlauf M, Depboylu C, Schafer MKH, Weihe E (2002) The vesicular monoamine transporters (VMATs): role in the chemical coding of neuronal transmission and monoamine storage in amine-handling immune and inflammatory cells. In Nagatsu T, Nabeshima T, Mc Carty R, Goldstein DS, eds. Catecholamine Research: From Molecular Insights to Clinical Medicine. Advances in Behavioural Biology. New York, Kluwer Academic Publishers 53:23–24

Eissele R, Anlauf M, Schäfer MKH, Eiden LE, Arnold R, Weihe E (1999) Expression of vesicular monoamine transporters in endocrine hyperplasia and endocrine tumors of the oxyntic stomach. Digestion 60:428–439

Erickson JD, Eiden LE (1993) Functional identification and molecular cloning of a human brain vesicle monoamine transporter. J Neurochem 61:2314–2317

Erickson JD, Eiden LE, Hoffman BJ (1992) Expression cloning of a reserpine-sensitive vesicular monoamine transporter. Proc Natl Acad Sci USA 89:10993–10997

Erickson JD, Schäfer MK, Bonner TI, Eiden LE, Weihe E (1996) Distinct pharmacological properties and distribution in neurons and endocrine cells of two isoforms of the human vesicular monoamine transporter. Proc Natl Acad Sci USA 93:5166–5171

Erickson JD, Varoqui H (2000) Molecular analysis of vesicular amine transporter function and targeting to secretory organelles. FASEB J 14:2450–2458

Fon EA, Pothos EN, Sun BC, Killeen N, Sulzer D, Edwards RH (1997) Vesicular transport regulates monoamine storage and release but is not essential for amphetamine action. Neuron 19:1271–1283

Furuzawa Y, Ohmori Y, Watanabe T (1994) Immunohistochemical colocalization of serotonin, aromatic L-amino acid decarboxylase and polypeptide hormones in islet A- and PP-cells of the cat pancreas. J Vet Med Sci 56:911–916

Hakanson R, Alumets J, Sundler F (1978) Classification of peptide-hormone-producing cells. Lancet 1:997

Hancock MB (1986) Two-color immunoperoxidase staining: visualization of anatomic relationships between immunoreactive neural elements. Am J Anat 175:343–352

Hansson SR, Mezey E, Hoffman BJ (1998) Ontogeny of vesicular monoamine transporter mRNAs VMAT1 and VMAT2. II. Expression in neural crest derivatives and their target sites in the rat. Brain Res Dev Brain Res 110:159–174

Hörsch D, Fink T, Büchler M, Weihe E (1993) Regional specificities in the distribution, chemical phenotypes, and coexistence patterns of neuropeptide containing nerve fibres in the human anal canal. J Comp Neurol 335:381–401

Iturriza FC, Thibault J (1993) Immunohistochemical investigation of tyrosine-hydroxylase in the islets of Langerhans of adult mice, rats and guinea pigs. Neuroendocrinology 57:476–480

Jakobsen AM, Andersson P, Saglik G, Andersson E, Kolby L, Erickson JD, Forssell–Aronsson E, et al. (2001) Differential expression of vesicular monoamine transporter (VMAT) 1 and 2 in gastrointestinal endocrine tumours. J Pathol 195:463–472

Jones PM, Fyles JM, Persaud SJ, Howell SL (1987) Catecholamine inhibition of Ca^{2+}-induced insulin secretion from electrically permeabilised islets of Langerhans. FEBS Lett 219:139–144

Komminoth P, Heitz PU, Roth J (1999) Human insulinomas: clinical, cellular, and molecular aspects. Endocr Pathol 10:269–281

Li Y, Hao Y, Zhu J, Owyang C (2000) Serotonin released from intestinal enterochromaffin cells mediates luminal non-cholecystokinin-stimulated pancreatic secretion in rats. Gastroenterology 118:1197–1207

Lindstrom P, Sehlin J (1983) Mechanisms underlying the effects of 5-hydroxytryptamine and 5-hydroxytryptophan in pancreatic islets. A proposed role for L-aromatic amino acid decarboxylase. Endocrinology 112:1524–1529

Liu Y, Peter D, Roghani A, Schuldiner S, Prive GG, Eisenberg D, Brecha N, et al. (1992) A cDNA that suppresses MPP+ toxicity encodes a vesicular amine transporter. Cell 70:539–551

Lundquist I, Ahren B, Hansson C, Hakanson R (1989) Monoamines in pancreatic islets of guinea pig, hamster, rat, and mouse determined by high performance liquid chromatography. Pancreas 4:662–667

Mahony C, Feldman JM (1977) Species variation in pancreatic islet monoamine uptake and action. Diabetes 26:257–261

Masuda M, Miyasaka K, Funakoshi A (1997) Involvement of 5-hydroxytryptamine (5-HT)3 receptor mechanisms in regulation of basal pancreatic secretion in conscious rats. J Auton Nerv Syst 62:58–62

Persaud SJ, Jones PM, Howell SL (1993) Activation of protein kinase C partially alleviates noradrenaline inhibition of insulin secretion. Biochem J 289:497–501

Peter D, Liu Y, Sternini C, De Giorgio R, Brecha N, Edwards RH (1995) Differential expression of two vesicular monoamine transporters. J Neurosci 15:6179–6188

Rausch DM, Heyes MP, Murray EA, Lendvay J, Sharer LR, Ward JM, Rehm S, et al. (1994) Cytopathologic and neurochemical correlates of progression to motor/cognitive impairment in SIV-infected rhesus monkeys. J Neuropathol Exp Neurol 53:165–175

Rindi G, Paolotti D, Fiocca R, Wiedenmann B, Henry JP, Solcia E (2000) Vesicular monoamine transporter 2 as a marker of gastric enterochromaffin-like cell tumors. Virchows Arch 436:217–223

Roth J, Kloppel G, Madsen OD, Storch MJ, Heitz PU (1992) Distribution patterns of proinsulin and insulin in human insulinomas: an immunohistochemical analysis in 76 tumors. Virchows Arch [B] 63:51–61

Roth J, Komminoth P, Heitz PU (1995) Topographic abnormalities of proinsulin to insulin conversion in functioning human insulinomas. Comparison of immunoelectron microscopic and clinical data. Am J Pathol 14:489–502

Schütz B, Schäfer MKH, Eiden LE, Weihe E (1998) Vesicular amine transporter expression and isoform selection in developing brain, peripheral nervous system and gut. Brain Res Dev Brain Res 106:181–204

Sener A, Blachier F, Rasschaert J, Malaisse WJ (1990) Stimulus-secretion coupling of arginine-induced insulin release: comparison with histidine-induced insulin release. Endocrinology 127: 107–113

Sjoholm A (1995) Histaminergic regulation of pancreatic beta-cell replication and insulin secretion. Biochem Biophys Res Commun 214:224–229

Solcia E, Klöppel G, Sobin LH, in collaboration with nine pathologists from four countries (2000) Histological Typing of Endocrine Tumours. 2nd ed. WHO International Histological Classification of Tumours. Berlin, Springer

Sundler F, Hakanson R (1988) Peptide hormone-producing endocrine/paracrine cells in the gastro-entero-pancreatic region. In Björklund A, Hökfeld T, Owman C, eds. Handbook of Chemical Neuroanatomy. Vol 6: The Peripheral Nervous System. Amsterdam, Elsevier, 219–295

Suzuki A, Naruse S, Kitagawa M, Ishiguro H, Yoshikawa T, Ko SB, Yamamoto A, et al. (2001) 5-hydroxytryptamine strongly inhibits fluid secretion in guinea pig pancreatic duct cells. J Clin Invest 108:749–756

Teitelman G, Alpert S, Polak JM, Martinez A, Hanahan D (1993) Precursor cells of mouse endocrine pancreas coexpress insulin, glucagon and the neuronal proteins tyrosine hydroxylase and neuropeptide Y, but not pancreatic polypeptide. Development 118:1031–1039

Walsh JH (1994) Gastrointestinal homones. In Johnson LR, Alpers DH, Jacobson ED, Christensen J, Walsh JH, eds. Physiology of the Gastrointestinal Tract. Vol 1. New York, Raven Press, 3–127

Weihe E, Eiden LE (2000) Chemical neuroanatomy of the vesicular amine transporters. FASEB J 14:2435–2449

Weihe E, Schäfer MKH, Erickson JD, Eiden LE (1994) Localization of vesicular monoamine transporter isoforms (VMAT1 and VMAT2) to endocrine cells and neurons in rat. J Mol Neurosci 5:149–164

Yajima H, Komatsu M, Sato Y, Yamada S, Yamauchi K, Sharp GW, Aizawa T, et al. (2001) Norepinephrine inhibits glucose-stimulated, Ca^{2+}-independent insulin release independently from its action on adenylyl cyclase. Endocr J 48:647–654